

## Bond Multiplicity in Transition-Metal Complexes: Applications of Two-Electron Valence Indices

Artur Michalak,<sup>\*,†</sup> Roger L. DeKock,<sup>‡,§</sup> and Tom Ziegler<sup>‡</sup>

Department of Theoretical Chemistry, Faculty of Chemistry, Jagiellonian University, R. Ingardena 3, 30-060 Cracow, Poland, Department of Chemistry, University of Calgary, 500 University Dr NW, Calgary, Alberta Canada, and Department of Chemistry and Biochemistry, Calvin College, 3201 Burton St SE, Grand Rapids, Michigan 49546

Received: January 8, 2008; Revised Manuscript Received: March 11, 2008

In the present study the applicability of the bond multiplicities from the Nalewajski and Mrozek valence indices was demonstrated for a variety of transition metal-based systems. The Nalewajski–Mrozek valence indices and bond multiplicity indices have been implemented in the Amsterdam Density Functional program. Selected examples comprise the carbonyl complexes (selected tetra- and hexacarbonyls, binary monocarbonyls of the first-row transition metals), phosphines, the ligands' trans-influence, as well as multiple metal–ligand and metal–metal bonds. The results show that the calculated bond multiplicity indices correspond well to experimental predictions based on bond lengths and vibrational frequencies for all discussed classes of complexes. Almost perfect linear correlation between the bond indices and vibrational frequencies was observed for carbonyls and the oxo complexes; the calculated bond multiplicity reproduces the accepted order for the trans-influence of different ligands, rationalizes unusually low vibrational frequencies in the  $[\text{OsO}_3\text{N}]^-$  complex compared to other nitrido complexes, explains the geometrical asymmetry in the  $\text{MoO}_3$  solid, and confirms the multiple character of the metal–metal bond in the  $[\text{Re}_2\text{Cl}_8]^{2-}$  complex. Thus, the Nalewajski and Mrozek method can be successfully used as a supplementary analysis tool for electronic structure for studies involving transition metal complexes.

### Introduction

“Chemical bonding” has always been “a traditional territory and heartland of chemistry”, as emphasized by Sason Shaik.<sup>1</sup> Both principal approaches of quantum chemistry, the valence bond theory and the molecular orbital theory, have contributed to understanding of the fundamental nature of the chemical bond in various molecular systems.<sup>2</sup> In particular, concepts such as atoms-in-molecules, chemical valence, and bond multiplicities have been considered since the very beginning of quantum chemistry. Although these quantities are not observables in the quantum-mechanical sense,<sup>3</sup> they provide a link between a rigorous description of electronic structure by quantum mechanics and the everyday language of chemistry (“classical” Lewis concepts,<sup>4</sup> structural formulas of the molecules, etc.). Therefore, they are often successfully used as supplementary tools in a discussion rationalizing the results of theoretical calculations.

A few alternative definitions of the valence and bond-indices have been proposed in the literature, starting from the pioneering attempts of Pauling,<sup>5,6</sup> Coulson,<sup>7</sup> and Wiberg,<sup>8</sup> through Jug,<sup>9</sup> Gopinathan,<sup>10</sup> Mayer,<sup>11,12</sup> Cioslowski and Mixon,<sup>13</sup> Glendenning and Weinhold,<sup>14</sup> up to the recently developed two- and three-electron indices of Nalewajski, Köster, Jug, and Mrozek.<sup>15–21</sup> Most recently, new approaches for a description of chemical bonds were proposed in the framework of information theory of molecular systems.<sup>22,23</sup>

A known problem for the most commonly used population analyses and popular bond indices is their basis set dependence

and their inadequacy in combination with extended basis sets. This introduces a limitation in their applicability to the problems involving transition metals, for which large basis sets (multiple-zeta, polarization functions) have to be used to provide a reasonable approximation for the wave function or electron density distribution within the *ab initio* methods. Here, the Nalewajski and Mrozek (N–M)<sup>16–21</sup> approach seems to be superior as it explicitly includes both, molecule and promolecule: described in the same basis sets. Thus, the approach that we will apply here allows one to use extended basis sets practically without an influence on the results.

N–M valence and bond indices have recently been implemented in the Amsterdam Density Functional (ADF) program.<sup>24</sup> A main purpose of the present study was to demonstrate the usefulness of the N–M<sup>16–21</sup> bond-multiplicity indices in a description of electronic structure of selected transition metal (TM) complexes. In inorganic and organometallic chemistry it is common to discuss the bond-strengthening/weakening in terms of the bond shortening/elongation or the positive/negative shifts in the vibrational frequencies for the bond-stretching modes. In the present work we will present the calculated N–M bond multiplicities for a variety of TM-based systems and confront the results with experimental data. The example set of TM complexes discussed here comprises the carbonyl complexes (selected tetra- and hexacarbonyls, binary monocarbonyls of the first row TMs), phosphines, the trans-influence of various ligands, as well as multiple metal–ligand and metal–metal bonds.

A few alternative definitions<sup>16–21</sup> of the two-electron valence indices have evolved from the pioneering work by Nalewajski, Köster, and Jug,<sup>15</sup> as well as Nalewajski and Mrozek.<sup>16</sup> Therefore, to avoid confusion we briefly summarize the alterna-

\* Corresponding author e-mail: michalak@chemia.uj.edu.pl.

<sup>†</sup> Jagiellonian University.

<sup>‡</sup> University of Calgary.

<sup>§</sup> Calvin College.

**TABLE 1: Alternative Definitions of the Nalewajski–Mrozek Valence Indices<sup>12–17</sup> Expressed in Terms of the Difference in Molecular and Promolecular CBO Matrices,  $\Delta\mathbf{P} = \mathbf{P} - \mathbf{P}^0$** 

valence index	set 1, two-electron 4-index set <sup>a</sup>	set 2; $V = 1/4 \text{ tr} (\Delta\mathbf{P}^2)$ 3-index set	set 3, $V = 1/2\text{tr} (P\Delta P)$ 3-index set
one-center			
$V_A^{(1),\text{ion}}$	$\frac{1}{2} \left[ -(\Delta n_A)^2 + \sum_a^A \{(\Delta P_{aa}^\alpha)^2 + (\Delta P_{aa}^\beta)^2\} \right]$ (1)	$\frac{1}{2} \sum_a^A \{(\Delta P_{aa}^\alpha)^2 + (\Delta P_{aa}^\beta)^2\}$ (5)	$\sum_a^A \{P_{aa}^\alpha \Delta P_{aa}^\alpha + P_{aa}^\beta \Delta P_{aa}^\beta\}$ (8)
$V_A^{(1),\text{cov}}$	$\sum_{a<}^A \sum_{a'}^A [(\Delta P_{aa'}^\alpha)^2 + (\Delta P_{aa'}^\beta)^2]$ (2)	$\sum_{a<}^A \sum_{a'}^A [(\Delta P_{aa'}^\alpha)^2 + (\Delta P_{aa'}^\beta)^2]$ (6)	$2 \sum_{a<}^A \sum_{a'}^A \{P_{aa'}^\alpha \Delta P_{a'a}^\alpha + P_{aa'}^\beta \Delta P_{a'a}^\beta\}$ (9)
two-center			
$V_{AB}^{(2),\text{ion}}$	$-\Delta n_A \Delta n_B$ (3)		
$V_{AB}^{(2),\text{cov}}$	$\sum_a^A \sum_b^B [(\Delta P_{ab}^\alpha)^2 + (\Delta P_{ab}^\beta)^2]$ (4)	$\sum_a^A \sum_b^B [(\Delta P_{ab}^\alpha)^2 + (\Delta P_{ab}^\beta)^2]$ (7)	$2 \sum_a^A \sum_b^B \{P_{ab}^\alpha \Delta P_{ba}^\alpha + P_{ab}^\beta \Delta P_{ba}^\beta\}$ (10)

$$^a - \Delta n_x = \sum_x^X (\Delta P_{xx}^\alpha + \Delta P_{xx}^\beta)$$

tive sets of N–M valence and bond multiplicity indices and comment on their physical meaning prior to the presentation of the results for the TM-systems.

**Theory and Computational Details. Nalewajski–Mrozek Valence Indices.** Two-electron valence indices have been originally defined by Nalewajski and Mrozek<sup>16</sup> by considering changes in the pair-diagonal part of the two-electron density matrix (i.e., two-electron probabilities) due to formation of the molecule from isolated atoms. For a single-determinantal wave functions they can be expressed in terms of the changes in the molecular and promolecular charge-and-bond-order (CBO) matrix (first-order density matrix),  $\Delta\mathbf{P} = \mathbf{P} - \mathbf{P}^0$ . A concept of promolecule has been introduced here as a species corresponding to the separated atom limit, constructed from noninteracting atoms placed in their molecular positions. Thus, a promolecular CBO matrix  $\mathbf{P}^0$  is built from atomic CBO matrices and contains vanishing interatomic (off-diagonal) blocks.

The original set of Nalewajski–Mrozek valence indices<sup>16</sup> is presented in the first column of Table 1 (1-4); we shall refer to these indices as Set 1. It comprises the one- and two-center contributions, both including the covalent ( $V_A^{(1),\text{cov}}$ ,  $V_{AB}^{(2),\text{cov}}$ ), as well as ionic ( $V_A^{(1),\text{ion}}$ ,  $V_{AB}^{(2),\text{ion}}$ ) indices.

The sum of all the contributions over all atoms/atom pairs leads to the overall valence value (eq 11),

$$V = \sum_A (V_A^{(1),\text{ion}} + V_A^{(1),\text{cov}}) + \sum_{A<} \sum_B (V_{AB}^{(2),\text{ion}} + V_{AB}^{(2),\text{cov}}) \quad (11)$$

apparently corresponding to the total number of all chemical bonds in the molecule.<sup>19,20</sup>

It was later shown by Nalewajski et al.<sup>19–21</sup> that the two-center ionic valence indices cancel with part of the one-center ionic valence indices, when the number of electrons in the molecule and promolecule is the same. Thus, another set of the valence indices corresponding to the same value of the overall valence can be considered; this set is listed in the second column of Table 1 (eqs 5–7); we shall refer to these indices as Set 2. This set of indices was used in the previous applications of the N–M theory.<sup>19–21</sup>

What follows from eqs 5-7 is that the overall valence can be expressed as a trace of the  $1/4 \Delta\mathbf{P}^2$  matrix. Further, it has been shown<sup>20</sup> for the spin-restricted case that

$$V = \frac{1}{4} \text{Tr}(\Delta\mathbf{P}^2) = \frac{1}{2} \text{Tr}(\mathbf{P}\Delta\mathbf{P}) \quad (12a)$$

For the spin-unrestricted case the analogous expression reads:

$$V = \frac{1}{2} \text{Tr}[(\Delta\mathbf{P}^\alpha)^2 + (\Delta\mathbf{P}^\beta)^2] = \text{Tr}[\mathbf{P}^\alpha \Delta\mathbf{P}^\alpha + \mathbf{P}^\beta \Delta\mathbf{P}^\beta] \quad (12b)$$

Thus, yet another alternative set of valence indices, corresponding to the same value of the overall valence  $V$ , arises from the right-hand side of 12a or 12b. This set is listed in the last column of Table 1 (eqs 8–10); we shall refer to these indices as Set 3. A decomposition of the total valence into the components of eqs 8–10 is shown in Appendix 1. In Appendix 2 we apply the valence indices of eqs 8–10 for the two-orbital bond model. It is shown in this appendix that the N–M scheme reproduces the expected, intuitive values of the bond multiplicities.

**Bond Multiplicity from the Valence Indices.** The valence indices of Table 1 include one- and two-center contributions. To construct bond multiplicity indices<sup>17,19–21</sup> from the valence indices one has to express the overall valence solely in terms of diatomic contributions,  $V = \sum_A \sum_B b_{AB}$ . This can be done by splitting the one-center index of an atom among the bonds that this atom forms. Thus, the bond multiplicity index can be calculated as a sum of the relevant two-center part and weighted contributions from one-center indices of the two atoms,<sup>19–21</sup>

$$b_{AB} = V_{AB}^{(2)} + w_A^{AB} V_A^{(1)} + w_B^{AB} V_B^{(1)} \quad (13)$$

with the weighting factors

$$w_X^{XY} = V_{XY}^{(2),\text{cov}} / \sum_Z V_{XZ}^{(2),\text{cov}} \quad (14)$$

Equation 13 can be applied for any of the alternative sets of the valence indices. In all the cases  $V^{(1)} = V^{(1),\text{ion}} + V^{(1),\text{cov}}$  and  $V^{(2)} = V^{(2),\text{cov}}$ , except for Set 1 for which  $V^{(2)} = V^{(2),\text{ion}} + V^{(2),\text{cov}}$ .

It should be pointed out that the way of dividing one-center terms is arbitrary; one can define weighting factors  $w_X^{XY}$  other than those of eq 14. In the present study we will apply the proportional weighting factors of eq 14, because they have been shown<sup>19–21</sup> to give bond multiplicities in agreement with commonly accepted values for typical molecules.

A comment on terminology seems to be desired at this point. It is common in chemistry to use the term “bond order”, when referring to bond multiplicity. The term bond order was first introduced by Coulson,<sup>7</sup> also, in fact, referring to bond multiplicity (“For a pure single bond such as ethane, the total order is 1; for a pure double bond such as ethylene, the total order is 2; for a pure triple bond such as acetylene, the total order is 3”). Original Coulson bond orders evaluated within molecular orbital approach are linear in density matrix elements. The N–M valence indices, and thus bond multiplicities, are quadratic. Therefore, to avoid any confusion, we will not use the term bond order in the present manuscript, using “bond multiplicity” or “bond index” instead. However, it should be emphasized that the calculated bond multiplicities correspond to values that are very often called bond orders in chemistry, see Appendix 2.

**Valence Operator and Relation to the Deformation Density,  $\Delta\rho$ .** The right-hand side of eq 12a or 12b allows one to formally identify<sup>20</sup> the overall valence ( $V$ ) as the expectation value of the valence operator  $\hat{V}$  in the basis  $\chi$ . Thus,

$$\mathbf{V} = \left\{ V_{ij} = \langle \chi_i | \hat{V} | \chi_j \rangle = \frac{1}{2} \Delta P_{ij} \right\} \quad (15)$$

since in the one-electron approximation

$$V = \frac{1}{2} \text{Tr}(\mathbf{P}\Delta\mathbf{P}) = \text{Tr}\left(\mathbf{P}\frac{1}{2}\Delta\mathbf{P}\right) = \text{Tr}(\mathbf{P}\mathbf{V}) = \langle \Psi | \hat{V} | \Psi \rangle = \langle \hat{V} \rangle \quad (16)$$

Thus, the valence operator can be formally written as the difference between the projection operators in the molecule and promolecule (eq 17).

$$\hat{V} = \frac{1}{2}(\hat{P} - \hat{P}^0) = \frac{1}{2}(\langle \psi | \langle \psi | - | \psi^0 \rangle \langle \psi^0 |) = \frac{1}{2} \left( \sum_i^{\text{MO}} | \psi_i \rangle \langle \psi_i | - \sum_j^{\text{MO}} | \psi_j^0 \rangle \langle \psi_j^0 | \right) \quad (17)$$

Such a definition of the chemical valence provides a link with another basic quantity, commonly used to diagnose and visualize the presence of a chemical bond: the deformation density (differential density),  $\Delta\rho$ .

$$\Delta\rho(r) = \sum_a \sum_b \Delta P_{ab} \chi_a^*(r) \chi_b(r) \quad (18)$$

**A Few Comments on the Arbitrariness and Basis-set Dependence.** One of the characteristics of the N–M theory is that chemical valence is formulated as the changes in electron pairing relative to a promolecular reference state. Thus, chemical valence is a differential property. The presence of the promolecular reference state obviously introduces arbitrariness in the approach as there is no unique way to define an atom in a molecule.<sup>3</sup> It should be emphasized, however, that this arbitrariness is in fact present in any approach; if one wants to define bonds between atoms, then this implies that one has to define atoms in a molecule. Although this problem is explicitly considered in the N–M approach, it is also present in the most popular Wiberg-related bond-index definitions (e.g., Gopinathan and Jug,<sup>10</sup> Mayer<sup>11</sup>). In these approaches an atom is identified

by the set of basis functions centered on its nucleus; this introduces a strong basis-set dependence of these definitions.

In the present work an atom is identified by its atomic Kohn–Sham orbitals and the corresponding  $\mathbf{P}^0$  matrix obtained from atomic calculations. Thus, it may be expected that the basis set dependence (through the basis set dependence of the atomic Kohn–Sham orbitals) should be less pronounced here.<sup>21</sup>

A further issue in defining bond multiplicity arises for ionic species. Namely, the bond indices will contain a contribution from the change in the number of electrons,  $\Delta N$  if a neutral (atomic) promolecule is assumed. This is a general problem with a choice of promolecule that exists in any differential approach, for example, in the case of the local density difference maps or contours, commonly used to visualize chemical bonds. However, it is worth emphasizing that the aforementioned contribution from the change in the number of electrons for ionic species is as well absorbed in other definitions of bond-multiplicity measures, for example, in the Gopinathan–Jug or Mayer approach, when the bond-indices are calculated based exclusively on the  $\mathbf{P}$  (or  $\mathbf{PS}$ ) matrix of the charged species.

Finally, the way in which one divides the one-center terms between bonds (eqs 13 and 14) is arbitrary. As a result, bond multiplicities calculated from the alternative sets of valence indices may be slightly different, because the one- and two-center contributions are different within each set, although they all give the same value of the overall valence  $V$ . This problem is more pronounced when the indices of Sets 1 and 2 are used then in the case of Set 3, as the divided one-center contributions are smaller in the latter definition. Thus, Set 3 originating from  $\text{Tr}(\mathbf{P}\Delta\mathbf{P})$  is least influenced by the arbitrariness in dividing one-center contributions.

**ADF Implementation.** In the present account we present the results obtained from our implementation of the N–M formalism into the ADF program.<sup>24–28</sup> The ADF program adopts a fragment-based approach in the DFT calculations. Namely, the Kohn–Sham orbitals of a molecular system are expressed in the basis of the symmetrized fragment orbitals (SFO), that is, the orthogonalized Kohn–Sham orbitals of smaller fragments. In standard calculations these fragments correspond to the atoms, that is, the basis consists of converged atomic Kohn–Sham orbitals calculated with the same computational details as for molecular calculations. Thus, unlike in other quantum chemical programs, calculating N–M valence indices does not require extra atomic calculations in ADF.

As in previous applications of the N–M theory,<sup>19–21</sup> we assume that the promolecule is built from noninteracting, isolated fragments. Thus, in the basis of the fragment Kohn–Sham orbitals, the promolecule CBO matrix is diagonal,  $P_{ij}^0 = 0$  and  $\Delta P_{ij} = P_{ij}$  for  $i \neq j$ .

For molecules built from the open-shell atoms, the one-center valence index is calculated as an average value from all equivalent electronic configurations of an atom. This is done by changing occupations of the open-shell orbitals, determined for average configuration with fractional occupations. Such an approach introduces a negligible error.<sup>21</sup>

**Computational Details.** In all DFT calculations the Becke–Perdew exchange-correlation functional<sup>29–31</sup> was used. A standard double- $\zeta$  STO basis with one set of polarization functions was applied for main-group elements (H, C, N, O, S), and a standard triple- $\zeta$  basis set was employed for the transition metals. The 1s electrons of C, N, O, 1s–2p electrons of P, S, as well as the 1s–2p (1s–3d) electrons of the first row (second row) transition metals were treated as frozen core. Auxiliary s, p, d, f, and g STO functions, centered on all nuclei, were used to fit

**TABLE 2: Calculated Bond Multiplicities and Experimental Vibrational Frequencies<sup>28</sup> for Carbon Monoxide**

species	configuration	frequency [cm <sup>-1</sup> ]	bond multiplicity
CO	(5σ) <sup>2</sup>	2143	3.04
CO <sup>+</sup>	(5σ) <sup>1</sup>	2184	3.21
CO* (triplet)	(5σ) <sup>1</sup> (2π) <sup>1</sup>	1715	2.66

the electron density and to obtain accurate Coulomb potential in each SCF cycle. The bond multiplicities calculated from the Set 2 N–M valence indices will be presented in the article. In general, Sets 2 and 3 lead to similar bond-multiplicity values, close to the chemist's intuition, whereas Set 1 often visibly differs from the other two, especially for charged species.

## Results and Discussion

In the following we will present the bond multiplicities calculated by the N–M method for selected transition-metal complexes. First the results for “classical” carbonyl complexes will be presented, then the trans influence of the ligands will be discussed, and, finally, examples of the complexes with the multiple metal–ligand and metal–metal bonds will be explored.

**Carbon Monoxide and the Binary Transition Metal–Carbonyls.** Carbonyl complexes are among the best-known transition metal-based systems; they are common starting material in the synthesis of other complexes and are also used as probes for determining the electronic structure of organometallic species.<sup>32</sup> Chemical bonding in transition metal–carbonyls has been extensively studied by numerous theoretical methods.<sup>33</sup>

The calculated bond-multiplicity values for the neutral ground-state of the carbon monoxide, its cation and the excited state (triplet) are collected in Table 2, together with the experimental values of the CO vibrational frequencies.<sup>32</sup> The CO molecule according to the N–M method has practically a “pure” triple bond (bond-index of 3.04). The method predicts an increase in the CO bond multiplicity in the cation (3.21) and a decrease in the excited state (2.66). Thus, calculated bond indices correctly reflect the trend observed in the experimental vibrational frequencies: 2143, 2184, 1715 cm<sup>-1</sup>, for the neutral CO, CO<sup>+</sup>, and triplet CO\*, respectively.

Figure 1 collects the calculated bond indices for the first row, neutral (MCO), cationic (MCO<sup>+</sup>), and anionic (MCO<sup>-</sup>) binary carbonyls of the first row transition metals. Experimental and theoretical data for these species have been discussed in detail in the review by Zhou, Andrews and Bauschlicher.<sup>34</sup> The CO bond in the binary carbonyls varies between “double” and “triple” bond (bond multiplicity changes from 2.1 in ScCO<sup>-</sup> to 2.8 in CuCO<sup>+</sup>). In the neutral binary carbonyls the CO bond multiplicity changes between 2.2 (ScCO) and 2.7 (CuCO); it

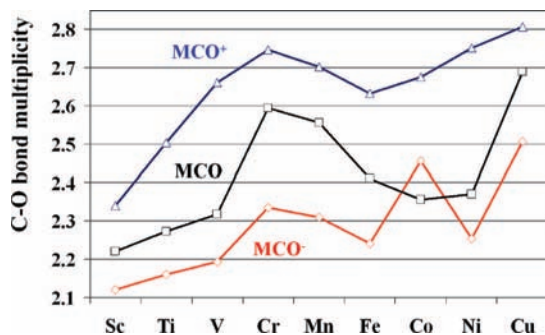


**Figure 1.** Calculated C–O bond multiplicities for neutral, cationic, and anionic binary carbonyl complexes of the first-row transition-metals.

**TABLE 3: Calculated Bond Multiplicities, Bond Lengths and Experimental Vibrational Frequencies<sup>28</sup> for CO Bonds in Selected Tetra- and Hexacarbonyl Complexes**

	species	frequency [cm <sup>-1</sup> ]	bond length [Å]	bond multiplicity
<i>d</i> <sup>10</sup>	Ni(CO) <sub>4</sub>	2060	1.150	2.52
	[Co(CO) <sub>4</sub> ] <sup>-</sup>	1890	1.176	2.26
	[Fe(CO) <sub>4</sub> ] <sup>-2</sup>	1790	1.207	2.06
<i>d</i> <sup>6</sup>	[Mn(CO) <sub>6</sub> ] <sup>+</sup>	2090	1.139	2.56
	Mo(CO) <sub>6</sub>	2010	1.154	2.46
	Cr(CO) <sub>6</sub>	2000	1.156	2.45
	[V(CO) <sub>6</sub> ] <sup>-</sup>	1860	1.178	2.24

**TABLE 4: Calculated Bond Multiplicities for CO Bond in Selected Ni(CO)<sub>3</sub>R Phosphines**

R	bond multiplicity
P(CH <sub>3</sub> ) <sub>3</sub>	2.43
P(C <sub>6</sub> H <sub>5</sub> ) <sub>3</sub>	2.44
P(OCH <sub>3</sub> ) <sub>3</sub>	2.45
P(OC <sub>6</sub> H <sub>5</sub> ) <sub>3</sub>	2.47
PCl <sub>3</sub>	2.51
PF <sub>3</sub>	2.51
CO	2.52

first increases from Sc to Cr (2.6) and then decreases from Cr to Ni (2.4) to reach a maximal value for CuCO (2.7). A similar trend is observed for cationic carbonyls. Here, however, the bond indices are, in general, higher than for neutral molecules, changing from 2.1 in ScCo<sup>+</sup> to 2.8 in CuCO<sup>+</sup>, with a local maximum for CrCO<sup>+</sup> (2.75). For anions, the minimal value is observed for ScCO<sup>-</sup> (2.1), with the maximal for CuCO<sup>-</sup> (2.5); the local maxima are obtained for CrCO<sup>-</sup> (2.3) and CoCO<sup>-</sup> (2.45). Figure 1 reproduces general features of the experimental CO vibrational frequencies collected in ref 27, the lowest frequency has been observed for ScCO<sup>-</sup> (1732 cm<sup>-1</sup>), and the highest for CuCO<sup>+</sup> (2230 cm<sup>-1</sup>); the experimental frequencies for neutral and charged species also exhibit an initial increase from Sc to Cr/V, followed by a decrease and local minimum.<sup>34</sup>

**Selected Tetra- and Hexacarbonyls of Transition Metals.** The calculated bond multiplicities for a series of tetrahedral *d*<sup>6</sup> tetracarbonyl complexes, Ni(CO)<sub>4</sub>, Co(CO)<sub>4</sub><sup>-</sup>, Fe(CO)<sub>4</sub><sup>-2</sup>, and selected octahedral *d*<sup>10</sup> hexacarbonyls, Mn(CO)<sub>6</sub><sup>+</sup>, Cr(CO)<sub>6</sub>, Mo(CO)<sub>6</sub>, Mn(CO)<sub>6</sub><sup>-</sup>, are collected in Table 3, together with experimental CO vibrational frequencies.<sup>32</sup> In a series of tetracarbonyls the CO bond index decreases from 2.4 for Ni to 2.0 for Fe; this reflects a decrease in the CO stretching frequencies (from 2060 to 1790 cm<sup>-1</sup>) observed experimentally. Similarly, for hexacarbonyls, the CO bond multiplicity is highest for Mn (2.6) and is lowest for V (2.2), as reflected by changes

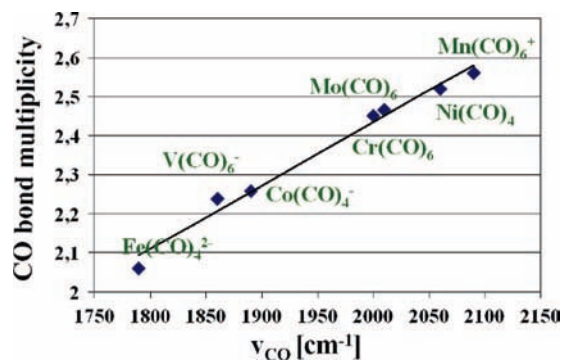


**Figure 2.** Calculated C–O bond multiplicities as a function of the experimental C–O stretching vibrational frequencies for selected tetra- and hexacarbonyl complexes. Experimental frequencies taken from ref.<sup>28</sup>

in experimental frequencies (from 2090 to 1860  $\text{cm}^{-1}$ ). The investigated complexes are collected in Figure 2, in the calculated bond multiplicity versus experimental CO frequency plot. The figure shows almost perfect linear correlation ( $R^2 = 0.99$ ) between CO bond indices and their stretching frequencies.

As should be expected, the changes in bond multiplicity are reflecting the changes in the bond-length. For the carbonyl complexes studied here we have included C–O distances in Table 3. The shortest CO bond in  $[\text{Mn}(\text{CO})_6]^+$  (1.139 Å) corresponds to the largest bond multiplicity (2.6), and the longest bond in  $[\text{Fe}(\text{CO})_4]^{-2}$  (1.206 Å) is characterized by the smallest value (2.1). Thus, the N–M scheme can be seen as a useful method for relating changes in bond-distances to changes in bond multiplicity. It is clear that the accuracy of geometry optimization will directly influence calculated values of bond indices.

Another “textbook” example of a well-known set of carbonyl complexes are the Tolman phosphines,  $\text{Ni}(\text{CO})_3(\text{PR}_3)$ .<sup>35–37</sup> The bond multiplicity calculated for this set are listed in Table 4. It is known from experimental trend in the CO stretching frequencies that the phosphine ligand decreases the CO bond multiplicity, the effect is highest for  $\text{R} = \text{P}(\text{CH}_3)_3 > \text{P}(\text{C}_6\text{H}_5)_3 > \text{P}(\text{OCH}_3)_3 > \text{P}(\text{OC}_6\text{H}_5)_3 > \text{PCl}_3 > \text{PF}_3$ .<sup>35–37</sup> Despite small variations in the CO bond indices in this series (2.43–2.50), the trend is still very well reproduced by calculated values for all the complexes.

Finally, we would like to address the issue of the basis set influence on the N–M bond multiplicities calculated for the transition metal complexes. Table 5 presents the values of the N–M bond indices for the example carbonyl complexes discussed above,  $\text{Ni}(\text{CO})_4$ ,  $\text{Cr}(\text{CO})_6$ , and the carbon monoxide molecule calculated with different basis set quality and the frozen core level; the Mayer bond-orders were, in addition, calculated for comparison. To exclude the effect of the geometry change, all the values in Table 5 were determined for the same geometry of a given molecule, optimized at the level applied in the preset study as default (TZP/1s–2p for the metal and DZP/1s for C, O). The results clearly show that there is a very small basis set effect. This is true for the values describing C–O bond as well as the metal–carbon bond. The calculated values of the N–M bond multiplicities are very stable with respect to basis set and the frozen core approximation; the variations in the N–M values are much smaller than for the Mayer bond

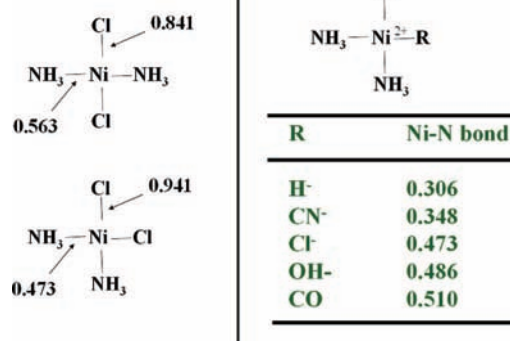


**Figure 3.** Calculated Ni–N and Ni–Cl bond multiplicities in the tetracarbonyl complexes illustrating the trans influence of the ligands.

orders; the latter approach appears to be quite sensitive for the changes in the frozen core level.

**The Trans Influence of the Ligands.** It is known that some ligands cause a more pronounced weakening of the bond in the trans position than other ligands; this effect is usually called the trans influence. The well-established order of the trans influence for different ligands is:  $\text{H}^- > \text{CN}^- > \text{Cl}^- > \text{OH}^- > \text{CO}$ ; here “>” indicates stronger trans influence, that is, larger weakening of the bond in the trans position.<sup>38,39</sup>

To demonstrate the usefulness of the N–M bond multiplicities in a description of the trans influence, we have performed DFT calculations for the two isomers of the square-planar  $[\text{Ni}(\text{NH}_3)_2\text{Cl}_2]^{2+}$  complex and the series of  $[\text{Ni}(\text{NH}_3)_2\text{L}_2]^{2+}$  complexes with  $\text{L} = \text{H}^-, \text{CN}^-, \text{Cl}^-, \text{OH}^-, \text{CO}$ . The results are presented in Figure 3.

Figure 3 shows the Ni–Cl and Ni–N bond multiplicities in the cis and trans isomers of  $[\text{Ni}(\text{NH}_3)_2\text{Cl}_2]^{2+}$ . The Ni–Cl bond index in the trans position to the  $\text{NH}_3$  ligand is 0.94, and in the trans position to another  $\text{Cl}^-$  ligand it is 0.84. Similarly, the Ni–N bond multiplicity in the trans position to the  $\text{NH}_3$  ligand is 0.56, and in the trans position to the  $\text{Cl}^-$  ligand it is 0.47. Thus, the  $\text{Cl}^-$  ligand causes a more pronounced weakening of the trans metal–ligand bond than the  $\text{NH}_3$  ligand.

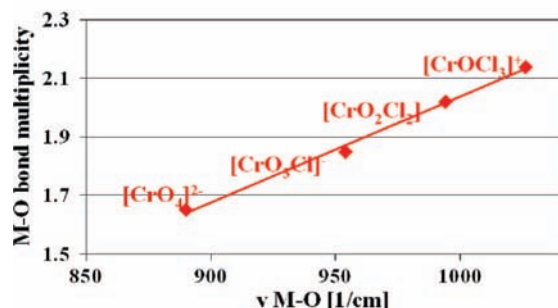
The table in Figure 3 lists the Ni–N bond in the trans  $[\text{Ni}(\text{NH}_3)_2\text{L}_2]^{2+}$  complexes with  $\text{L} = \text{H}^-, \text{CN}^-, \text{Cl}^-, \text{OH}^-$ , and

**TABLE 5: Basis Set Dependence of the N–M Bond Multiplicities for  $\text{Ni}(\text{CO})_4$ ,  $\text{Cr}(\text{CO})_6$  and CO; Mayer Bond Multiplicities Are Shown for Comparison**

molecule <sup>a</sup>	basis set/frozen core level		C–O bond multiplicity		metal–C bond multiplicity	
	C, O	metal	N–M	Mayer	N–M	Mayer
$\text{Ni}(\text{CO})_4$	TZP/all el.	TZP/all el.	2.54	2.24	0.56	1.01
	DZP/all el.	TZP/all el.	2.52	2.14	0.56	0.96
	DZ/all el.	TZP/all el.	2.50	2.12	0.57	0.95
	SZ/all el.	TZP/all el.	2.52	2.40	0.66	1.00
	DZP/1s	TZP/1s–2p	2.52	1.83	0.55	0.75
	DZP/1s	TZP/1s–3p	2.54	1.91	0.53	0.80
$\text{Cr}(\text{CO})_6$	TZP/all el.	TZP/all el.	2.47	2.15	0.80	0.98
	DZP/all el.	TZP/all el.	2.46	2.11	0.81	0.87
	DZ/all el.	TZP/all el.	2.43	2.10	0.80	0.86
	SZ/all el.	TZP/all el.	2.44	2.33	0.83	1.02
	DZP/1s	TZP/1s–2p	2.45	1.88	0.81	0.49
	DZP/1s	TZP/1s–3p	2.47	1.91	0.81	0.54
CO	TZP/all el.		3.05	2.34		
	DZP/all el.		3.04	2.28		
	DZ/all el.		3.02	2.18		
	SZ/all el.		2.97	2.58		
	DZP/1s		3.04	2.15		
	DZ/1s		3.01	2.08		

<sup>a</sup> For each case the same geometry was used, optimized with TZP/1s–2p basis for the metal and DZP/1s for CO basis set/frozen core level.

Complex	$\nu_{(\text{Cr-O})}$	$b_{(\text{Cr-O})}$
$[\text{CrO}_4]^{2-}$	846, 890	1.65
$[\text{CrO}_3\text{Cl}]^-$	907, 954	1.85
$[\text{CrO}_2\text{Cl}_2]$	984, 994	2.02
$[\text{CrOCl}_3]^+$	1026*	2.14

\*  $\text{Cr}(\text{O})\text{Cl}$  (TPP) value

**Figure 4.** Calculated Cr–O bond multiplicities in the oxo-complexes  $[\text{CrO}_n\text{Cl}_{4-n}]^-$ ,  $n = 1, 4$ . Experimental frequencies are taken from ref 36.

CO. The Ni–N bond-index is smallest for the  $[\text{Ni}(\text{NH}_3)_2\text{H}_2]$  complex (0.31) and strongest for  $[\text{Ni}(\text{NH}_3)_2(\text{CO})_2]^{2+}$  (0.51). The trend of the calculated Ni–N bond multiplicity corresponds to the known trans influence ligands' order:  $\text{H}^- > \text{CN}^- > \text{Cl}^- > \text{OH}^- > \text{CO}$ .

#### Multiple Metal–Ligand Bonds: Oxo and Nitrido Complexes.

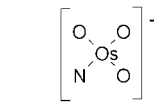
As examples of the multiple metal–ligand bonds, the metal–oxygen and metal–nitrogen bond multiplicities in the selected oxo and nitrido complexes will be discussed here. The first set are the chromium complexes  $[\text{CrO}_n\text{Cl}_{4-n}]^{2-}$ ,  $n = 1, 4$ . Figure 4 summarizes calculated Cr–O bond indices and the experimental<sup>40</sup> Cr–O vibrational frequencies. The Cr–O bond multiplicity changes between 1.65 for tetra-oxo species and 2.14 for the mono-oxo complex. The increasing number of oxygen ligands results in weakening of the metal–oxygen bond, in agreement with experimental results. Again, the bond multiplicity versus frequency plot exhibit almost perfect linear correlation ( $R^2 = 0.995$ ).

As another example of the metal–oxygen multiple bonds, we present the osmium oxo-nitrido complex  $[\text{OsO}_3\text{N}]^-$ , Figure 5. For this system, unusually low Os–N vibrational frequencies were experimentally observed.<sup>39</sup> The calculated Os–N and Os–O bond-indices are 2.18 and 1.49, respectively. Thus, the Os–N bond is rather a double bond, than a triple bond. Thus, the calculated bond multiplicities explains the relatively low experimental frequency of the metal–nitrogen bond. For comparison, we present the results for other osmium nitrido complexes,  $[\text{OsBr}_4\text{N}]^-$ ,  $[\text{OsCl}_4\text{N}]^-$ , and  $[\text{OsCl}_5\text{N}]^-$ . In these complexes the metal–nitrogen bond multiplicity is ca. 2.9 (triple bond), and the frequencies vary between  $1073 \text{ cm}^{-1}$  and  $1123 \text{ cm}^{-1}$ . Here, small changes in the calculated bond indices (2.85, 2.87, and 2.89, for  $[\text{OsBr}_4\text{N}]^-$ ,  $[\text{OsCl}_4\text{N}]^-$ , and  $[\text{OsCl}_5\text{N}]^-$ , respectively) do not reflect the variation in the frequencies (1119, 1123, and  $1073 \text{ cm}^{-1}$ , in the same order). However, the qualitative difference between  $[\text{OsO}_3\text{N}]^-$  and the remaining systems demonstrate the usefulness of the N–M bond multiplicities in a description of the metal–ligand multiple bonds.

#### Metal–Oxygen Bonds in the Molybdenum Trioxide Solid.

An interesting example of the variation in the metal–oxygen bonds is the crystal structure of  $\text{MoO}_3$  (Figure 6a) in which the

Complex	$\nu_{(\text{Os-N})}$	$b_{(\text{Os-N})}$
$[\text{OsBr}_4\text{N}]^-$	1119	2.85
$[\text{OsCl}_4\text{N}]^-$	1123	2.87
$[\text{OsCl}_5\text{N}]^-$	1073	2.89



Os–O 1.49  
Os–N 2.18  
exp.  $\nu_{(\text{Os-N})} = 844.826 \text{ cm}^{-1}$

**Figure 5.** Calculated Os–N bond multiplicities in the selected nitrido complexes. Experimental frequencies are taken from ref 36.

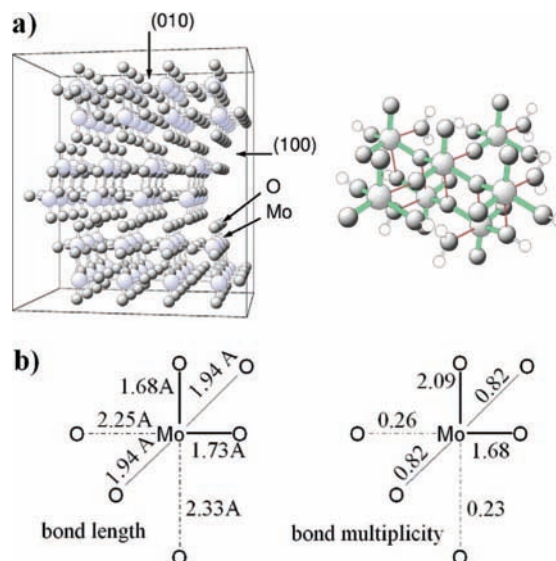


**Figure 6.** Structure of  $\text{MoO}_3$  and the cluster modeling the (010)- $\text{MoO}_3$  surface (panel a). Mo–O bond-lengths and the corresponding N–M bond multiplicities (panel b)

octahedral coordination around the metal is strongly distorted, leading to three types of metal–oxygen bonds, characterized by short (1.68, 1.73 Å), intermediate (1.94 Å), or long (2.25, 2.33 Å) Mo–O distances.<sup>41</sup> The N–M Mo–O bond indices calculated for the cluster model of  $\text{MoO}_3$ ,  $\text{Mo}_7\text{O}_{30}\text{H}_{18}$ , used in previous studies,<sup>42</sup> are shown in Figure 6b. The bond multiplicity changes from 1.7 and 2.1 for the shortest bonds (double), through 0.8 (single), down to 0.2 (weak ionic interactions). This picture is fully consistent with the deformation-density maps (differential density) previously published<sup>42</sup> that clearly differentiate the three types of Mo–O interactions.

**Multiple Metal–Metal Bonds.** Multiple metal–metal bonds have attracted special attention in the literature and lead to many controversies.<sup>43–49</sup> As the simplest molecule exhibiting the metal–metal multiple bond we studied  $\text{Cr}_2$ , for which the N–M method gives the bond-index of 6.01. This comes as a result of the  $d^5s^1$  electronic configuration of Cr, leading to the two  $\sigma$ , two  $\pi$ , and two  $\delta$  components of the bond in  $\text{Cr}_2$ .

Among the most controversial system is the  $[\text{Re}_2\text{Cl}_8]^{2-}$  complex (Figure 7), discovered by Cotton in the 1960s, for which the quadruple Re–Re bond was postulated.<sup>43–45</sup> The metal–metal bond multiplicity in this system has been the subject of many recent theoretical studies.<sup>46–49</sup> Here we have applied the N–M bond-index to describe the metal–metal bond in the  $[\text{Re}_2\text{Cl}_8]^{2-}$  complex and related systems:  $[\text{Mo}_2\text{Cl}_8]^{4-}$ ,  $[\text{Cr}_2\text{Cl}_8]^{4-}$ , and  $[\text{Re}_2\text{H}_8]^{2-}$  complexes.

The metal–metal bond-multiplicity values calculated for the aforementioned complexes are listed in Figure 7. The Re–Re bond index in  $[\text{Re}_2\text{Cl}_8]^{2-}$  is 2.9 (triple bond). In the related molybdenum and chromium complexes the corresponding value

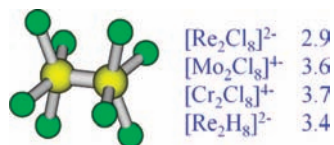


**Figure 7.** Calculated metal–metal bond multiplicities in the selected complexes (atomic resolution, atom–atom bond indices, see text).

is much larger (3.6, 3.7), approaching that of a quadruple bond. In the  $[\text{Re}_2\text{H}_8]^{2-}$  complex in the eclipsed conformation the bond multiplicity is increased to 3.4. This indicates that a weakening of the Re–Re bond in  $[\text{Re}_2\text{Cl}_8]^{2-}$  results from a competition between Cl ligands and the other metal for the metal  $\pi$ -orbitals.

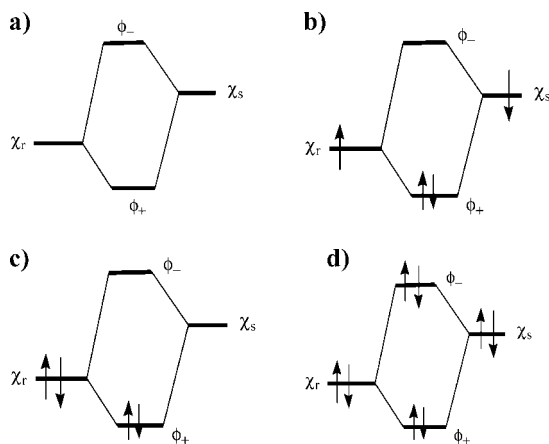
**Concluding Remarks.** In this study we have applied the N–M bond-multiplicity indices, as implemented into the ADF program, to a description of chemical bonding in various transition metal complexes. The differential nature of the N–M bond indices makes them less sensitive to extended basis sets as both molecule and promolecule are described in the same basis. Further, this approach includes both covalent and ionic contributions. The results demonstrate that this methodology indeed leads to bond multiplicities that correspond to chemical intuition. Further, computed bond multiplicities exhibit the trends reflecting changes in experimental vibrational frequencies. The N–M method is, in addition, useful in translating the changes in bond distances into variations in bond multiplicities. Thus, it may be concluded that the N–M bond-indices can be very useful as a supplementary tool for the analysis of the electronic structure of transition metal-based systems.

**Acknowledgment.** This work was supported by a research grant from the Ministry of Education and Science in Poland (1130-T09-2005-28). T. Z. thanks the Canadian Government for a Canada Research Chair. R. D. K. thanks the Donors of the American Chemical Society Petroleum Research Fund for partial support of this research.

## Appendix 1

**Derivation of the  $\mathbf{P}\Delta\mathbf{P}$ -based Valence Indices.** Let us first assume the spin-restricted case. The overall valence,  $V$ , given by  $\frac{1}{2}\text{Tr}(\mathbf{P}\Delta\mathbf{P})$  may be decomposed as:

### SCHEME A1: Two-orbital Bond Model



$$\begin{aligned}
 \frac{1}{2}\text{Tr}\mathbf{P}\Delta\mathbf{P} &= \frac{1}{2}\sum_a\sum_b P_{ab}\Delta P_{ba} \\
 &= \frac{1}{2}\sum_A\sum_a\sum_{a'} P_{aa'}\Delta P_{a'a} + \\
 &\quad \sum_{A<B}\sum_a\sum_b P_{ab}\Delta P_{ba} \\
 &= \frac{1}{2}\sum_A\left\{\sum_a P_{aa}\Delta P_{aa} + 2\sum_{a<a'}\sum_{a'} P_{aa'}\Delta P_{a'a}\right\} + \\
 &\quad \sum_{A<B}\sum_a\sum_b P_{ab}\Delta P_{ba} \\
 &= \sum_A\left\{\frac{1}{2}\sum_a P_{aa}\Delta P_{aa} + \sum_{a<a'}\sum_{a'} P_{aa'}\Delta P_{a'a}\right\} + \\
 &\quad \sum_{A<B}\sum_a\sum_b \left\{\sum_a\sum_b P_{ab}\Delta P_{ba}\right\} \\
 &\equiv \sum_A V_A^{(1)} + \sum_{A<B}\sum_B V_{AB}^{(2)} \quad (\text{A1})
 \end{aligned}$$

In the spin-unrestricted case the contributions from both spin-components have to be included. An analogous decomposition leads to the indices defined by 8–10 (Table 1). It should be pointed out that in the spin-unrestricted equations the factor of 2 appears, compared to the spin-restricted indices of eq A1, since, for the spin-restricted case  $\mathbf{P} = \mathbf{P}^\alpha + \mathbf{P}^\beta = 2\mathbf{P}^\alpha = 2\mathbf{P}^\beta$  and  $\Delta\mathbf{P} = \Delta\mathbf{P}^\alpha + \Delta\mathbf{P}^\beta$ , and thus

$$\begin{aligned}
 \text{Tr}(\mathbf{P}^\alpha\Delta\mathbf{P}^\alpha + \mathbf{P}^\beta\Delta\mathbf{P}^\beta) &= \text{Tr}\left(\left[\frac{1}{2}\mathbf{P}\right]\Delta\mathbf{P}^\alpha + \left[\frac{1}{2}\mathbf{P}\right]\Delta\mathbf{P}^\beta\right) \\
 &= \text{Tr}\left(\left[\frac{1}{2}\mathbf{P}\right][\Delta\mathbf{P}^\alpha + \Delta\mathbf{P}^\beta]\right) = \text{Tr} \\
 &\quad \left(\frac{1}{2}\mathbf{P}\Delta\mathbf{P}\right) = \frac{1}{2}\text{Tr}(\mathbf{P}\Delta\mathbf{P}) \quad (\text{A2})
 \end{aligned}$$

## Appendix 2

**Two-orbital Bond Model.** In a “classical” molecular orbital picture for the two-orbital system (Scheme A1), two molecular orbitals  $\phi^+$ ,  $\phi^-$  (four spin-orbitals,  $\phi^{+, \alpha}$ ,  $\phi^{+, \beta}$ ,  $\phi^{-, \alpha}$ ,  $\phi^{-, \beta}$ ) are expressed as a combination of two atomic (fragment) orbitals,  $\chi_x$ ,  $\chi_s$ :

$$\varphi^{+, \sigma} = \sin\theta\chi_r^\sigma + \cos\theta\chi_s^\sigma, \quad \varphi^{-, \sigma} = -\sin\theta\chi_r^\sigma + \cos\theta\chi_s^\sigma, \quad \sigma = \alpha, \beta \quad (\text{A3})$$

The intuitive way of defining the bond multiplicity is as the difference in the bonding and antibonding electron-pairs:  $b = (n - n^*)/2$ . In the following we consider the typical two-orbital cases, shown in Scheme A1, calculating the N–M bond indices as follows.

$$\begin{aligned}
 \text{Tr}(\mathbf{P}^\alpha\Delta\mathbf{P}^\alpha + \mathbf{P}^\beta\Delta\mathbf{P}^\beta) &= P_{r,r}^\alpha\Delta P_{r,r}^\alpha + P_{r,r}^\beta\Delta P_{r,r}^\beta + P_{s,s}^\alpha\Delta P_{s,s}^\alpha + \\
 &\quad P_{s,s}^\beta\Delta P_{s,s}^\beta + P_{r,s}^\alpha\Delta P_{r,s}^\alpha + P_{r,s}^\beta\Delta P_{r,s}^\beta + P_{s,r}^\alpha\Delta P_{s,r}^\alpha + P_{s,r}^\beta\Delta P_{s,r}^\beta \quad (\text{A4})
 \end{aligned}$$

**Two Noninteracting (Nonbonding) Orbitals (Scheme A1a).** In this case  $\cos(\theta) = 1$ ,  $\sin(\theta) = 0$ , and  $P_{r,r}^\alpha = P_{r,r}^{\alpha,0} = 1$ ,  $P_{r,r}^\beta = P_{r,r}^{\beta,0} = 1$ ;  $P_{s,x}^\sigma = P_{s,x}^{\sigma,0} = 0$  for  $x = r, s$  and  $\sigma = \alpha, \beta$ . Thus, each element of the  $\Delta\mathbf{P}$  matrix is 0, and the bond multiplicity of eq A4 is  $b = 0$ .

**Two-orbital Two-electron Bond (Scheme A1b).** In this case  $0 < \cos \theta < 1$ , and  $0 < \sin \theta < 1$ . Thus,  $P_{r,r}^{\alpha} = P_{r,r}^{\beta} = \cos^2 \theta$ ,  $P_{s,s}^{\alpha} = P_{s,s}^{\beta} = \sin^2 \theta$  and  $P_{r,s}^{\alpha} = P_{s,r}^{\alpha} = P_{r,s}^{\beta} = P_{s,r}^{\beta} = \sin \theta \cos \theta$ .

In the diagram of Scheme A1b, both atomic orbitals were initially occupied by one electron with opposite spin,  $P_{r,r}^{\alpha,0} = P_{s,s}^{\beta,0} = 1$ , and the remaining elements of the promolecular  $\mathbf{P}^{\alpha,\sigma}$  vanish. This leads to the following values of  $\Delta\mathbf{P}$  matrix:  $\Delta P_{r,r}^{\alpha} = \cos^2 \theta - 1$ ,  $\Delta P_{r,r}^{\beta} = \cos^2 \theta$ ,  $\Delta P_{s,s}^{\alpha} = \sin^2 \theta$ ,  $\Delta P_{s,s}^{\beta} = \sin^2 \theta - 1$ , and  $\Delta P_{r,s}^{\alpha} = \Delta P_{s,r}^{\alpha} = \Delta P_{r,s}^{\beta} = \Delta P_{s,r}^{\beta} = \sin \theta \cos \theta$ . Using this values, expression A4 leads to the bond multiplicity  $b = 1$ , in agreement with the intuitive description.

**Two-electron Dative Bond (Scheme A1c).** The elements of the molecular  $\mathbf{P}^{\alpha}$  and  $\mathbf{P}^{\beta}$  matrices are the same as in the previous case. However, in this case we assume that in the promolecule both electrons are located in one atomic orbital. For example, in the case of the diagram of Scheme A1c:  $P_{r,r}^{\alpha,0} = P_{r,r}^{\beta,0} = 1$  and  $P_{s,s}^{\alpha,0} = P_{s,s}^{\beta,0} = 0$ . Thus, the  $\Delta\mathbf{P}$  matrix has the following elements:  $\Delta P_{r,r}^{\alpha} = \cos^2 \theta - 1$ ,  $\Delta P_{r,r}^{\beta} = \cos^2 \theta - 1$ ,  $\Delta P_{s,s}^{\alpha} = \sin^2 \theta$ ,  $\Delta P_{s,s}^{\beta} = \sin^2 \theta$ , and  $\Delta P_{r,s}^{\alpha} = \Delta P_{s,r}^{\alpha} = \Delta P_{r,s}^{\beta} = \Delta P_{s,r}^{\beta} = \sin \theta \cos \theta$ . With such a definition of the promolecule, eq A4 leads to bond index  $b = 2(1 - \cos^2 \theta)$ .

It can be easily shown that assuming both electrons initially located on the other orbital (Scheme A1d), that is,  $P_{s,s}^{\alpha,0} = P_{s,s}^{\beta,0} = 1$  and  $P_{r,r}^{\alpha,0} = P_{r,r}^{\beta,0} = 0$ , leads to bond index  $b = 2(1 - \sin^2 \theta)$ .

Thus, although in Schemes A1b–d the same bonding molecular orbital is doubly occupied, we obtained different bond multiplicity values for three sets of initial occupations of atomic orbitals,  $b = 1$ ,  $b = 2(1 - \cos^2 \theta)$ , or  $b = 2(1 - \sin^2 \theta)$ , for (1,1), (0,2), and (2,0) occupations on the two atomic orbitals, respectively. It may seem to be a bit problematic that the bond index depends on the initial occupations. However, this example nicely emphasizes the intrinsic dependence of the N–M bond multiplicities on the reference state. The meaning of “bond” is different in the three cases: it is either the bond between atoms or the bond between ions. Any quantitative description of the bond depends on what is bound by this bond. This is analogous to the bond dissociation energy, for instance, that obviously depends on the assumed dissociation limit (radical, ionic, etc.).

**Two-orbital Four-electron Case (Scheme A1d).** In this case  $0 < \cos \theta < 1$  and  $0 < \sin \theta < 1$ , both bonding and antibonding orbital are doubly occupied. Thus,  $P_{r,r}^{\alpha} = P_{r,r}^{\beta} = \cos^2 \theta + \sin^2 \theta = 1$ ,  $P_{s,s}^{\alpha} = P_{s,s}^{\beta} = 1$  and  $P_{r,s}^{\alpha} = P_{s,r}^{\alpha} = P_{r,s}^{\beta} = P_{s,r}^{\beta} = 0$ . In the promolecule, both atomic orbitals are doubly occupied,  $P_{r,r}^{\alpha,0} = P_{r,r}^{\beta,0} = P_{s,s}^{\alpha,0} = P_{s,s}^{\beta,0} = 1$ , so all the elements of the  $\Delta\mathbf{P}$  matrix vanish, and the total bond multiplicity is 0, in agreement with the intuitive value.

## References and Notes

- (1) Shaik, S. *J. Comput. Chem.*, **2007**, *28*, 51.
- (2) Hoffmann, R.; Shaik, S.; Hiberty, P. C. *Acc. Chem. Res.*, **2003**, *36*, 750.
- (3) Parr, R. G.; Ayers, P. W.; Nalewajski, R. F. *J. Phys. Chem. A* **2005**, *109*, 3957.
- (4) Lewis, G. N. *J. Am. Chem. Soc.* **1916**, *38*, 762.
- (5) Pauling, L.; Brockway, L. O.; Beach, J. Y. *J. Am. Chem. Soc.* **1935**, *57*, 2705.
- (6) Pauling, L. *The Nature of the Chemical Bond*, Cornell University Press, Ithaca, 1960, p 234.
- (7) Coulson, C. A. *Proc. Roy. Soc. Lond. A* **1939**, *169*, 413.
- (8) Wiberg, K. *Tetrahedron* **1968**, *24*, 1083.
- (9) Jug, K. *J. Am. Chem. Soc.* **1977**, *99*, 7800.
- (10) Gopinathan, M. S.; Jug, K. *Theoret. Chim. Acta* **1983**, *63*, 497.
- (11) Mayer, I. *J. Chem. Phys. Lett.* **1984**, *97*, 270.
- (12) Mayer, I. *J. Comput. Chem.* **2007**, *28*, 244–251.
- (13) Ciosłowski, J.; Mixon, S. T. *J. Am. Chem. Soc.* **1991**, *113*, 4142.
- (14) Glendenning, E. D.; Weinhold, F. *J. Comput. Chem.* **1998**, *19*, 610.
- (15) Nalewajski, R. F.; Köster, A. M.; Jug, K. *Theor. Chim. Acta* **1993**, *85*, 463.
- (16) Nalewajski, R. F.; Mrozek, J. *Int. J. Quantum Chem.* **1994**, *51*, 187.
- (17) Nalewajski, R. F.; Mrozek, J.; Formosinho, S. J.; Varandas, A. J. C. *Int. J. Quantum Chem.* **1994**, *52*, 1153.
- (18) Nalewajski, R. F.; Mrozek, J. *Int. J. Quantum Chem.* **1996**, *57*, 377.
- (19) Nalewajski, R. F.; Mrozek, J.; Mazur, G. *Can. J. Chem.* **1996**, *74*, 1121.
- (20) Nalewajski, R. F.; Mrozek, J.; Michalak, A. *Int. J. Quantum Chem.* **1997**, *61*, 589.
- (21) Nalewajski, R. F.; Mrozek, J.; Michalak, A. *Pol. J. Chem.* **1998**, *72*, 1779.
- (22) Nalewajski, R. F.; Jug, K. Information Distance Analysis of Bond Multiplicities in Model Systems, In *Reviews in Modern Quantum Chemistry: A Celebration of Contributions of Robert G. Parr*, Sen, K. Ed.; World-Scientific: Singapore, 2002; pp 148–203. Vol. I.
- (23) Nalewajski, R. F. *Information Theory of Molecular Systems*; Elsevier Science: Amsterdam, 2006.
- (24) TeVelde, G.; Bickelhaupt, F. M.; Baerends, E. J.; Fonseca Guerra, C.; Van Gisbergen, S. J. A.; Snijders, J. G.; Ziegler, T. *J. Comput. Chem.* **2001**, *22*, 931 and refs therein.
- (25) Baerends, E. J.; Ellis, D. E.; Ros, P. *Chem. Phys.* **1973**, *2*, 41.
- (26) Baerends, E. J.; Ros, P. *Chem. Phys.* **1973**, *2*, 52.
- (27) te Velde, G.; Baerends, E. J. *J. Comput. Phys.* **1992**, *99*, 84.
- (28) Fonseca, C. G.; Visser, O.; Snijders, J. G.; te Velde, G.; Baerends, E. J. In *Methods and Techniques in Computational Chemistry*, METECC-95; Clementi, E., Corongiu, G., Eds.; STEF: Cagliari, Italy, 1995; p 305.
- (29) Becke, A. *Phys. Rev. A* **1988**, *38*, 3098.
- (30) Perdew, J. P. *Phys. Rev. B* **1986**, *34*, 7406.
- (31) Perdew, J. P. *Phys. Rev. B* **1986**, *33*, 8822.
- (32) Elschenbroich, C., *Organometallics*. 3rd ed., Wiley: Weinheim, 2006, and refs therein.
- (33) Frenking, G.; Frohlich, N. *Chem. Rev.* **2000**, *100*, 717, and refs therein.
- (34) Zhou, M.; Andrews, L.; Bauschlicher, C. W. *Chem. Rev.* **2001**, *101*, 1931.
- (35) Tolman, C. A. *J. Am. Chem. Soc.* **1970**, *92*, 2656.
- (36) Tolman, C. A. *J. Am. Chem. Soc.* **1970**, *92*, 2953.
- (37) Tolman, C. A. *Chem. Rev.* **1977**, *77*, 313.
- (38) Crabtree, R. H. *The Organometallic Chemistry of Transition Metals*; Wiley: New Jersey, 1994.
- (39) Cotton, F. A.; Wilkinson, G. *Advanced Inorganic Chemistry*; Wiley: New York, 1988.
- (40) Nugent, W. A.; Mayer, J. M., *Metal–Ligand Multiple Bonds*; Wiley: New York, 1988; and refs therein.
- (41) Kihlborg, L. *Ark. Kemi* **1963**, *21*, 357.
- (42) Michalak, A.; Hermann, K.; Witko, M. *Surf. Sci.* **1996**, *366*, 323.
- (43) Krapp, A.; Lein, M.; Frenking, G. *Theor. Chem. Acc.* **2008**, *120*, 313.
- (44) Cotton, F. A. et al. *Science* **1964**, *145*, 1305.
- (45) Cotton, F. A. *Inorg. Chem.* **1965**, *4*, 330.
- (46) Frenking, G. *Science* **2005**, *310*, 796.
- (47) Gagliardi, L.; Roos, B. O. *Inorg. Chem.* **2003**, *42*, 1599.
- (48) Ponec, R.; Yuzhakov, G. *Theor. Chem. Acc.* **2007**, *118*, 791.
- (49) Krapp, A.; Lein, M.; Frenking, G. *Theor. Chem. Acc.* **2008**, *120*, 313–320.